

Measurement of the Noise Resistance for Corrosion Applications

A. Aballe,* A. Bautista,** U. Bertocci, and F. Huet***

ABSTRACT

Measurement of the noise resistance (R_n) or frequency-dependent noise impedance (Z_n), both derived from the fluctuations of current and voltage of electrodes corroding at the open-circuit potential, is more and more widespread for corrosion applications. These quantities have been shown to be related, under certain conditions, to the corrosion rate of the material under investigation. This type of measurement was proposed originally for a symmetric cell with identical electrodes, and much of its analysis has been based on the validity of this assumption. However, it is common that initially symmetrical cells become asymmetrical as a result of unequal corrosion of the electrodes. Also, a number of researchers have used asymmetrical cells to limit the corrosion phenomena to a single electrode, but the exact meaning of the measured values of R_n and Z_n is still questionable. To clarify the interpretation of electrochemical noise measurements, the experiments carried out in the laboratory on symmetric or asymmetric configurations were reviewed here. Results of the measurements of R_n and Z_n are discussed and explained on the basis of a theoretical model previously published.

KEY WORDS: asymmetric cell, current transient, electrochemical noise, monitoring, noise impedance, noise resistance, symmetric cell, voltage transient

Submitted for publication April 2000; in revised form, September 2000. Presented as paper no. 424 at CORROSION/2000, March 2000, Orlando, FL.

* Grupo de Investigación de Corrosión, Universidad de Cádiz, Puerto Real 11510, Spain.

** Centro Nacional de Investigaciones Metalúrgicas (CSIC), Madrid 28040, Spain.

*** UPR 15 du CNRS "Physique des Liquides et Electrochimie," Université Pierre et Marie Curie, 4 place Jussieu, 75252 Paris Cedex 05, France.

INTRODUCTION

Electrochemical noise (EN) measurements on a single corroding electrode give some important information about the electrochemical processes occurring but do not permit the corrosion rate to be obtained. For this purpose, Eden, et al., introduced the use of a cell with two identical working electrodes (WE) (same material, same size, same surface preparation), connected with a zero-resistance ammeter (ZRA), so as to have the same open-circuit potential, from which it was possible to obtain the noise resistance (R_n), defined as the ratio of the standard deviations of the voltage and current fluctuations.¹ Values of R_n were found to be close to the polarization resistance (R_p) so that the corrosion rate could be deduced by means of the Stern-Geary relationship.²

The possibility of obtaining the electrode impedance modulus from the voltage and current fluctuations was recently demonstrated theoretically and experimentally.³⁻⁵ The formulation of the model was sufficiently general to allow the treatment of asymmetrical cells, although both the discussion and most of the experimental results presented in these papers emphasized symmetrical systems.

Asymmetrical systems, however, are interesting first of all because corroding electrodes, particularly if the corrosion is localized, tend to develop differently even if the initial conditions are the same, and secondly because a number of researchers have proposed the use of asymmetrical cells, where only one electrode is corroding, the other being a cathode. For example, Chen and Bogaerts replaced one of the elec-

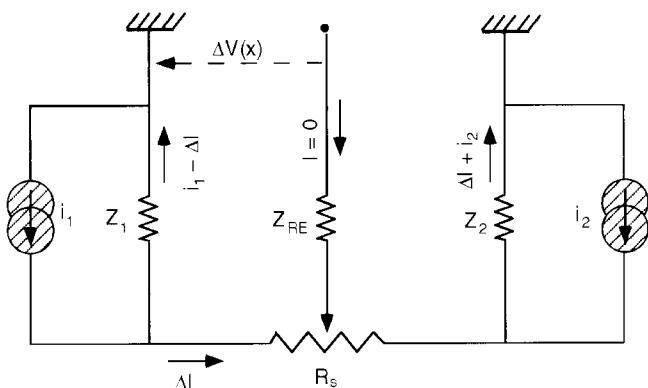


FIGURE 1. Equivalent circuit for a cell with two current-measuring electrodes and a noiseless RE.

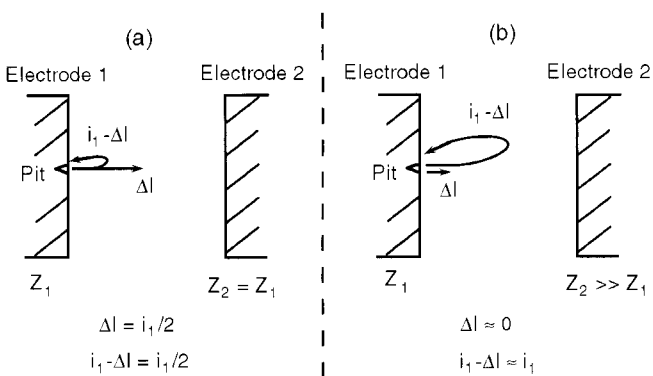


FIGURE 2. Distribution of the current i_1 produced by a pit on Electrode 1 for: (a) symmetric electrodes and (b) asymmetric electrodes, $Z_1 \ll Z_2$. The solution resistance was neglected.

trodes with a Pt microcathode,⁶ while others applied a voltage bias between two otherwise identical electrodes.⁷ The significance of the results obtained on asymmetrical cells, and therefore their relevance for corrosion studies, is still open to question. To clarify their interpretation, experiments were carried out in the laboratory on symmetric or asymmetric configurations and are reviewed here. Results of the measurements are discussed and explained on the basis of a theoretical model presented in a previous publication.³ To simplify the treatment, it will be assumed that the approximations of a "noiseless" reference electrode (RE) and a negligible solution resistance are valid. For a more detailed analysis of these points, the reader should consult previous works.^{3,8}

THEORY

The equivalent circuit representing the corrosion cell is given in Figure 1, where i_1 and i_2 are the current noise sources, in many cases associated with localized phenomena such as bubble formation and detachment, metastable or stable pitting, or crack advance. They are not directly measurable. Only

the fluctuations of the current (ΔI) flowing between the two electrodes and the coupled electrode potential (ΔV) are accessible to measure. The purpose of the equivalent circuit is to describe the dynamic behavior of a system around its mean; hence, it applies for all two-WE cell configurations, that is, for symmetric or asymmetric electrodes, with or without the superimposition of a bias voltage between the two electrodes.

Applying Ohm's law to the equivalent circuit, one can write, in the frequency domain:

$$\Delta I(f) = \frac{Z_1(f)i_1(f) - Z_2(f)i_2(f)}{Z_1(f) + Z_2(f)} \quad (1)$$

$$\Delta V(f) = -\frac{Z_1(f)Z_2(f)}{Z_1(f) + Z_2(f)} [i_1(f) + i_2(f)] \quad (2)$$

where $i_1(f)$, $i_2(f)$, $\Delta I(f)$, and $\Delta V(f)$ are the Fourier transforms of the time-dependent quantities $i_1(t)$, $i_2(t)$, $\Delta I(t)$, and $\Delta V(t)$, respectively. From these equations, it is possible to understand how the current generated by the corrosion of one electrode is partitioned between the two electrodes. Considering the case of a corrosion event occurring on Electrode 1, generating a current i_1 while nothing happens on Electrode 2 ($i_2 = 0$), from Equation (1), it is clear that for identical electrodes at the same potential ($Z_1 = Z_2$), only one half of i_1 flows to the other electrode, and therefore it is measured by the ZRA (Figure 2). On the contrary, if $Z_1 \ll Z_2$, almost all the current returns on Electrode 1, and the ZRA measures only a very small part of the current generated by the corrosion.

Since Equations (1) and (2) are written in the frequency domain, the derivation of the noise impedance (Z_n , called spectral noise impedance [R_{ni}] in previous publications) from the power spectral densities (PSD) of the voltage and current fluctuations is straightforward:

$$Z_n(f) = \sqrt{\frac{\Psi_v(f)}{\Psi_i(f)}} = |Z_1(f)Z_2(f)| \sqrt{\frac{\Psi_{i_1}(f) + \Psi_{i_2}(f)}{|Z_1(f)|^2 \Psi_{i_1}(f) + |Z_2(f)|^2 \Psi_{i_2}(f)}}} \quad (3)$$

As Equation (3) shows, Z_n depends on four parameters: the noise level of each electrode, expressed by its PSD Ψ_{i_1} , Ψ_{i_2} , and the impedance of each electrode, Z_1 and Z_2 . However, for two electrodes with the same impedance ($Z_1 = Z_2 = Z$), Z_n is equal to the modulus of the electrode impedance:

$$Z_n(f) = |Z(f)| \quad (4)$$

As Equation (3) shows, if $Z_1 = Z_2$, Equation (4) is valid whatever the origin of the noises (localized or uniform corrosion, bubble evolution) and the shape of the impedance plot, even if the noise levels of the two electrodes represented by ψ_{i1} and ψ_{i2} are different. Therefore, the knowledge of Z_n is equivalent to the knowledge of the modulus of the impedance for the purpose of obtaining the corrosion rate.

Equation (3) also can be used to discuss the case of asymmetrical cells, where $Z_1 \neq Z_2$, and ψ_{i1} and ψ_{i2} may differ. The various cases can be represented by Figure 3. In this figure, it is possible to study how the relative values of Z_1 vs Z_2 and ψ_{i1} vs ψ_{i2} determine whether Z_n is close to Z_1 , Z_2 , or none of them. To this end, in Figure 3, the independent variable is taken as the ratio $|Z_1|/|Z_2|$, and the results are represented by the ratio $Z_n/|Z_2|$, having as parameter the ratio ψ_{i1}/ψ_{i2} . If the values fall on the horizontal axis (defined at value 1), $Z_n = |Z_2|$. If the values fall on the diagonal through the origin, $|Z_n| = |Z_1|$. Unless $\psi_{i1}/\psi_{i2} > 1$ when $|Z_1|/|Z_2| < 1$ (or vice versa), Z_n tends to be close to the impedance of the less noisy electrode, even if it is the lowest impedance—a result that may appear counterintuitive since the equivalent circuit shows the two impedances in series. Hence, in a qualitative way, one can say that the noise of one electrode is the input signal for measuring the impedance of the other. However, all the quantities in Equation (3) are functions of the frequency, so that a conclusion valid for a certain frequency range may not be valid for another, as some of the examples presented in the following section show. Another general result illustrated by Figure 3 is that Z_n can never exceed the larger of the two impedances or be lower than the smaller one.

Another quantity, of more widespread use, employed to infer the corrosion rate from EN measurements is the R_n . This is usually calculated in the time domain as the ratio of the standard deviations of the voltage and current fluctuations, but, through a well-known mathematical relationship between standard deviations and PSD it can be expressed in the following form:

$$R_n = \frac{\sigma_v}{\sigma_i} = \sqrt{\frac{\int_{f_{\min}}^{f_{\max}} \Psi_v(f) df}{\int_{f_{\min}}^{f_{\max}} \Psi_i(f) df}} \quad (5)$$

which becomes:

$$R_n = \sqrt{\frac{\int_{f_{\min}}^{f_{\max}} \Psi_i(f) |Z(f)|^2 df}{\int_{f_{\min}}^{f_{\max}} \Psi_i(f) df}} \quad (6)$$

for identical electrodes at the same potential. As shown by Equation (6), two additional variables influence its value, the integration limits f_{\min} and f_{\max} . If Z

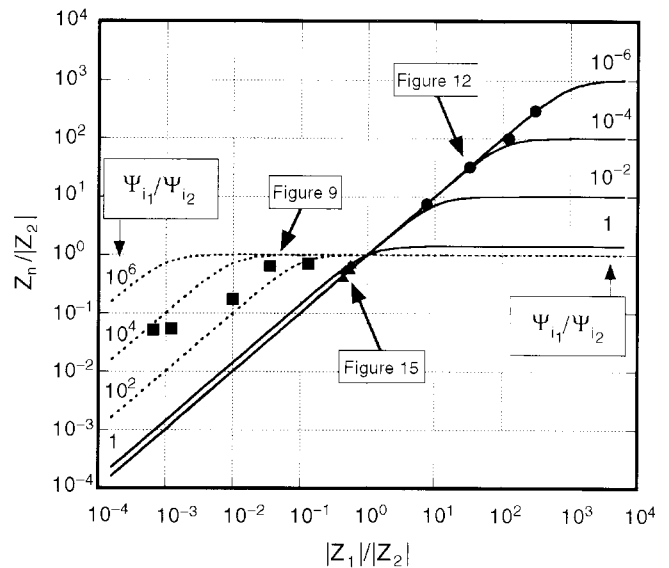


FIGURE 3. Ratio $Z_n/|Z_2|$ vs $|Z_1|/|Z_2|$, according to Equation (3), for various ratios ψ_{i1}/ψ_{i2} of the current noises. Some points calculated at various frequencies from experimental data in Figures 9, 12, and 15 are given.

and ψ are arbitrary functions of the frequency, Equation (6) shows that R_n is in no simple way related to the electrode impedance, so as to be used to obtain the corrosion rate. The reason R_n is in many cases close to the polarization resistance (zero frequency limit of the electrode impedance, often indicated as R_p) is that, in the frequency range between f_{\min} and f_{\max} , Z and ψ tend to be decreasing functions of the frequency. The outcome depends on the interplay between f_{\min} , the slope of the current PSD ψ_i , and the frequency at which the electrode impedance modulus reaches the low-frequency asymptote R_p . This is an important point that determines the usefulness of the measurement of R_n . It can be discussed with Figure 4, where this interplay is represented in normalized form, by two variables, f_c/f_{\min} and R_n/R_p . The quantity, f_c can be determined by Equation (7):

$$f_c = \frac{1}{2\pi R_p C} \quad (7)$$

is the critical frequency beyond which the impedance modulus $|Z|$ of a parallel circuit, consisting of a capacitance (C) and a resistance R_p , significantly decreases. From the figure, one can estimate when R_n will start to depart significantly from R_p , given the slope of the PSD, which was assumed to be constant between f_{\min} and f_{\max} , and the duration of the time record, which determines f_{\min} . When the slope of $\log \psi_i \geq -2$, time records for which $f_c/f_{\min} > 10$, that is, with a duration higher than $100 R_p C$ may be sufficient in many cases to estimate R_p from R_n . However, if R_p is very high (passive or coated electrodes), R_n

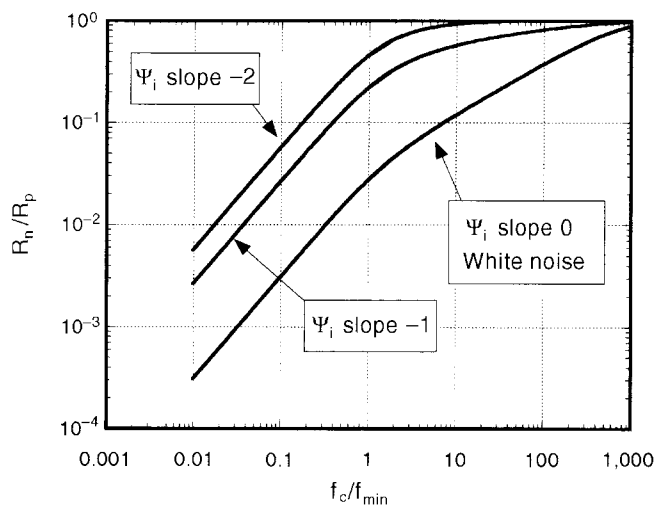


FIGURE 4. Ratio R_n/R_p as a function of the f_c of a R_p/C impedance. The slope of $\log \psi_i$ is taken constant between f_{min} and f_{max} ($f_{max}/f_{min} = 1,024$).

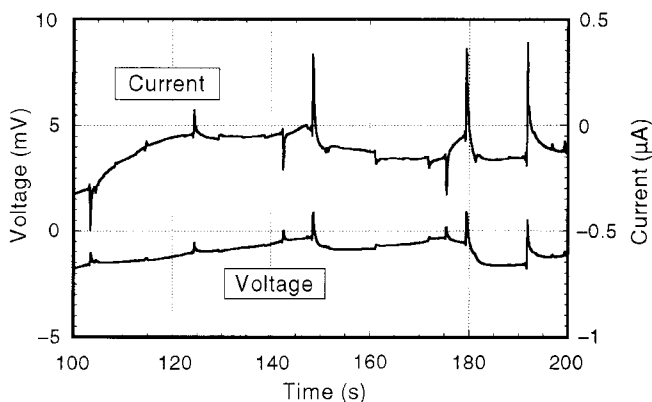


FIGURE 5. Time record of the voltage and current fluctuations for Fe in 1 M Na_2SO_4 at pH 3. Electrode area: 0.2 cm^2 . RE = saturated sulfate electrode. Zeros of scales are arbitrary.

may be substantially lower than R_p ,^{4,5,9} unless very long time records are taken, so as to satisfy the condition $f_c/f_{min} > 10$.

Similar considerations may be put forward for asymmetrical systems since Equation (6) may be rewritten:

$$R_n = \sqrt{\frac{\int_{f_{min}}^{f_{max}} \Psi_i(f) |Z_n(f)|^2 df}{\int_{f_{min}}^{f_{max}} \Psi_i(f) df}} \quad (8)$$

but it is difficult to give general results since R_n depends on too many parameters. As a corollary of the fact that Z_n has a value between the larger and the smaller of the two electrode impedance moduli at any frequency, it can be shown that, if $|Z_1|$ and $|Z_2|$ reach the polarization resistances R_{p1} and R_{p2} in the frequency range (f_{min}, f_{max}), the value of R_n is also

bounded by the values of the two polarization resistances. Moreover, if R_{p1} and R_{p2} are not too different, R_n will be equal to the polarization resistance of the less noisy electrode.⁹

RESULTS AND DISCUSSION

A number of examples drawn from results obtained in the laboratory will be presented and discussed here. The description of the experimental setup and measurement techniques were omitted, and the interested reader should consult the original papers.^{4,8-9}

Symmetrical Cells

An example of a symmetrical system is given by two identical Fe electrodes in sodium sulfate (Na_2SO_4) at pH = 3. The uniform corrosion generates H_2 bubbles, which are the main cause of noise. The time records of Figure 5 show simultaneous transients in the current (I) and voltage (V), which correspond to bubble detachment. The current transients occur in both directions, depending on which electrode they originate from, while the voltage transients are all in the same positive direction, since the detaching of the bubble causes a transient increase of the cathodic component of the current.

The PSD curves in Figure 6 show the beginning of a low-frequency plateau, followed by a decrease with more than one slope. Z_n , calculated from these curves, is in good agreement with the modulus of the impedance, measured with a three-electrode cell (Figure 7). Although the fluctuations are only indirectly related to the corrosion process, Z_n gives $|Z|$ as predicted by Equation (4). Since the modulus of the impedance (Figure 7) reaches the low-frequency asymptote R_p at a frequency much higher than f_{min} , R_n , calculated from the standard deviations σ_v and σ_i , is equal to R_p .

To show that, in the case of electrodes having the same impedance, the current generated by a localized corrosion event divides approximately equally onto each electrode, measurements were carried out on a cell constituted of two circular Type 316 L stainless steel electrodes (1.5 cm in diameter) immersed in a 0.06-M sodium chloride (NaCl) solution. In one, a hole was drilled to place in it a 250- μm diameter Fe wire insulated from the stainless steel. The three electrodes were kept at the same potential by three ZRA, so that it was possible to simultaneously measure the current on each electrode.¹⁰ The impedance of the composite electrode, stainless steel + Fe wire, was found to be approximately equal to that of the original stainless steel electrode.

Because of the anodic character of the Fe with respect to the stainless steel, corrosion soon occurred on it, and, because of the special circuit, it was possible to verify that the current transients

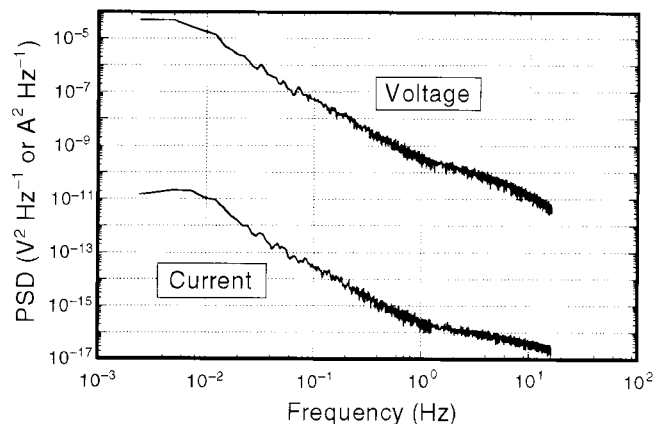


FIGURE 6. PSD of voltage and current noise for Fe in 1 M Na_2SO_4 at pH 3. Electrode area: 0.2 cm^2 . RE = saturated sulfate electrode.

generated in it flowed in equal quantities on the two stainless steel electrodes. the slight dissymmetry caused by the solution resistance being negligible. Results are presented in Figure 8, where it can be seen that the current on the Fe wire was composed of anodic transients, double in amplitude of the cathodic transients on the two stainless steel electrodes.

Asymmetrical Cells

A first example of asymmetrical systems with $Z_1 \neq Z_2$ is given when there is a large difference in size between the two electrodes. If the electrodes are otherwise identical, their impedances are inversely proportional to the surface area, while the current noise is directly proportional to it, as was demonstrated in an example previously presented (Figure 12 in Reference 4). Their behavior, therefore, can be understood by means of Equation (3). The treatment is simple: calling k the surface area ratio, it is $Z_1 = Z_2/k$, and $\psi_1 = k\psi_2$. Substituting into Equation (3), it is easily found that $Z_n = \sqrt{|Z_1| |Z_2|}$, the geometric mean of the moduli of the electrode impedances.

Asymmetrical systems of corroding electrodes often develop spontaneously when random corrosion events on one of the electrodes decrease its impedance, so that, by positive feedback, this electrode corrodes much more rapidly than the other.^{9,11} To accelerate the occurrence of asymmetry, in the following example, the electrodes had oxide surface layers of different thicknesses. The electrodes were of unsealed anodized Al, and the oxide thickness was $5 \mu\text{m}$ (Electrode 1) and $22 \mu\text{m}$ (Electrode 2). After 1 day in solution, impedances of the two electrodes were very different, as shown in Figure 9. The one with a thin oxide was extensively corroded, and its impedance was close to that of bare Al.⁹ The explanation of the Z_n curve can be understood by means of Figure 3. The corroding Electrode 1 was noisier, so that the ratio ψ_1/ψ_2 was between 10^3 and 10^4 .⁹ However, the ratio $|Z_1|/|Z_2|$ increased from 10^{-3} to 1

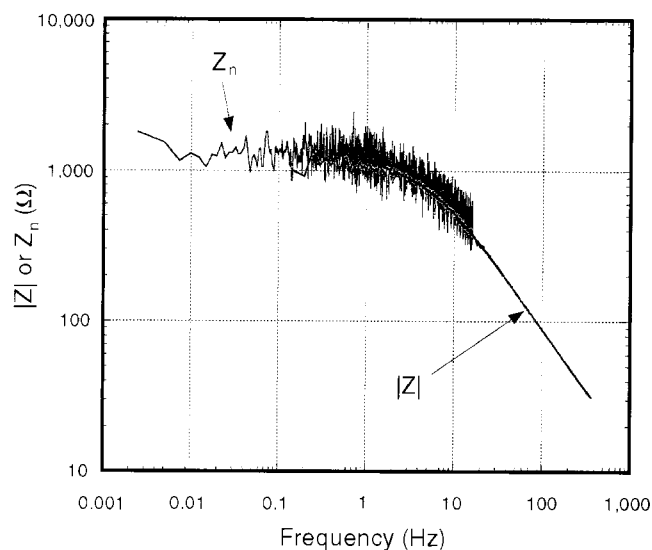


FIGURE 7. Z_n and $|Z|$ for Fe in 1 M Na_2SO_4 at pH 3. Z_n calculated from PSD in Figure 6. Impedance measurements performed with a three-electrode cell.

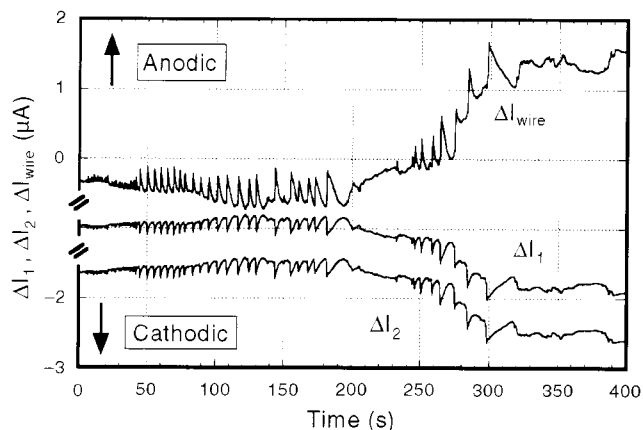


FIGURE 8. Time records of the current fluctuations. ΔI_{wire} , generated by corrosion of an Fe wire (diameter: $250 \mu\text{m}$) inserted in one of the two Type 316 L stainless steel electrodes (diameter: 1.5 cm), in a 0.06-M NaCl solution. ΔI_1 and ΔI_2 are the corresponding fluctuations of the currents crossing Electrode 1 and Electrode 2, respectively. Zeros of scales are arbitrary.

with increasing frequency (Figure 9). The ratio $Z_n/|Z_2|$ then moves in Figure 3 from the origin at high frequency approximately along the curve with parameter $\psi_1/\psi_2 = 10^3$. Therefore, at frequency $> 10 \text{ Hz}$, $Z_n = |Z_2|$ while at low-frequency Z_n takes a value intermediate between $|Z_1|$ and $|Z_2|$.

The asymmetric cell suggested by Chen and Bogaerts⁶ to have only one corroding electrode has the WE coupled to a Pt microelectrode, making both Z and ψ_i different. The effect of the coupling on the WE can be examined with the help of Figure 10. Between the Pt cathode and the WE flows a current, which tends to displace the potential of the WE in the anodic direction. However, if the surface area of the

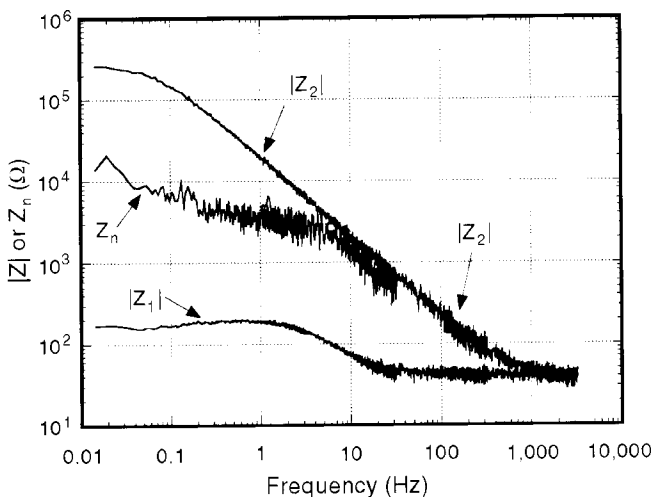


FIGURE 9. Impedance moduli and Z_n for two unsealed anodized Al electrodes with coating thickness of $5\ \mu\text{m}$ (Electrode 1) and $22\ \mu\text{m}$ (Electrode 2) after 1 day in $0.5\ \text{M NaOH} + 0.27\ \text{M NaCl}$ corrosive solution at pH 11. Surface area = $12.6\ \text{cm}^2$. RE = saturated calomel electrode.

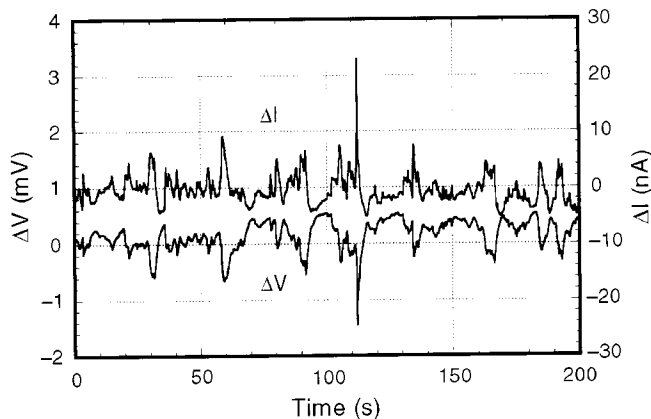


FIGURE 11. Time records of the voltage and current fluctuations generated during pitting corrosion of an Al disk (diameter: $2.5\ \text{cm}$) connected to a Pt disk (diameter: $1\ \text{mm}$) through a ZRA in $1\ \text{M KCl}$. Zeros of scales are arbitrary.

microcathode is small, this displacement is negligible, and the WE can be considered to be at the corrosion potential.

EN measurements on such a system also can be discussed in light of Equation (3). Depending on the material of the WE and the nature of the cathodic reaction, one can envisage different cases. Calling the Pt Electrode 1 and the WE Electrode 2, if the WE undergoes uniform corrosion and H_2 bubbles evolve on the Pt, the strong screening effect of the bubbles on the microcathode will produce a current noise i_1 much higher than that caused by the uniform corrosion of the WE. Hence, $\psi_{i_1}/\psi_{i_2} \gg 1$. $|Z_1|$ may also be greater than $|Z_2|$ because of the small size of the cathode, so that $|Z_1|/|Z_2| > 1$. As Figure 3 shows, in these conditions, Z_n is close to $|Z_2|$, making possible

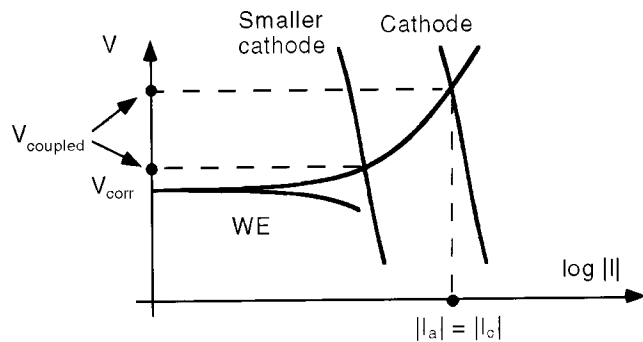


FIGURE 10. Current-voltage curves showing the coupled potential of a corroding WE and a small Pt cathode connected through a ZRA.

the measurement of the impedance of the WE, as an example in Reference 12 shows.

Opposite conditions are possible, as when the WE undergoes localized corrosion while dissolved O is reduced on the microcathode. In that case, the measurement of Z_n yields only the impedance of the microelectrode, as illustrated in the following example. In the realization of this system in the laboratory, the WE was an Al disk (diameter: $2.5\ \text{cm}$) coupled to a Pt disk (diameter: $1\ \text{mm}$) through a ZRA and immersed in $1\ \text{M}$ potassium chloride (KCl). In this case, the current noise was high on the Al because of pitting, as demonstrated by the voltage and current transients in opposite directions in the time records (Figure 11), while O reduction on the Pt generated little noise. As shown in Figure 12, the impedance of the Pt electrode was 10 to 100 times that of the Al. Calling the Pt Electrode 1 and the Al Electrode 2, the points corresponding to this system fall on the diagonal in Figure 3, showing that $|Z_n| = |Z_1|$. This was confirmed experimentally. The curve of Z_n coincides with the impedance modulus of the Pt microcathode (Figure 12). Hence, while the type of corrosion on the WE can be obtained from the shape of the transients in the time records, nothing concerning the WE can be inferred from Z_n .

Another type of asymmetrical system is obtained by applying a bias voltage (V_{bias}) between the two electrodes, so that only one is corroding.^{4,7} As shown in Figure 13, the two electrodes are no longer at the corrosion potential. In these conditions, the ZRA-potentiostat maintains a fixed V_{bias} , but, in case of instabilities or changes in the impedance of the electrodes, neither the potential of each electrode nor the current flowing is kept constant. Here, too, the noise current may be high on the anode (localized corrosion, for instance) or on the cathode (bubble evolution). Impedances also may differ, so that their ratio may be larger or smaller than 1. If the information is available, Equation (3) can be used and the position of Z_n mapped on Figure 3.

The example presented in this paper concerns uniform corrosion of a low-carbon steel electrode in

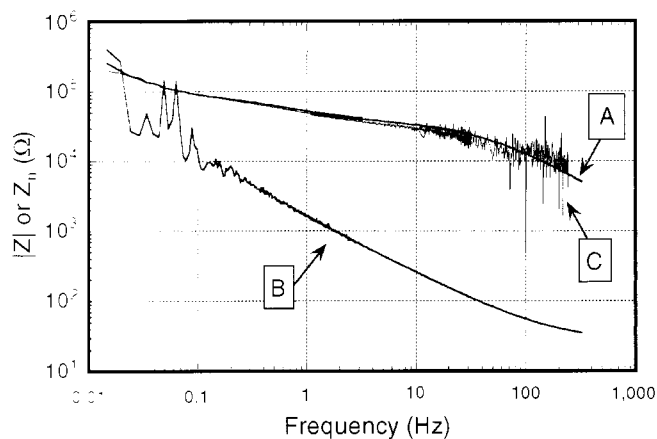


FIGURE 12. Impedance moduli of the: (A) Pt disk, (B) Al disk, and (C) noise impedance measured in the conditions of Figure 11.

0.1 M citric acid ($C_6H_8O_7$) with a V_{bias} of 350 mV. Most of the noise came from hydrogen bubble evolution on the cathode, as shown by the steep jumps followed by a linear decrease in the voltage and current time records (Figure 14). The anode underwent uniform corrosion, generating low noise, but, from time to time, hydrogen bubbles detached from the anode causing fast transients in the current noise source (i_a). However, these transients could not be clearly observed on the time records (Figure 14) because of the high noise generated by hydrogen evolution on the cathode and also because a great part of the current i did not cross to the other electrode, but returned back, in the manner explained in Figure 2 when $Z < Z_c$.

Figure 15 shows the impedance moduli of Electrode 1 ($|Z_a|$) and Electrode 2 ($|Z_c|$), as well as the noise impedance. For frequencies < 1 Hz, $Z_n = |Z_a|$. This is in agreement with theory since one can deduce from Equation (3) (or Figure 3) that $\psi_1 \gg \psi_2$ entails $Z_n = |Z_a|$. Hence, although the time records give information only on hydrogen evolution and nothing concerning the corrosion of the anode, monitoring Z_n gave information about the impedance of the anode. In other words, the anode impedance was measured using the noise of the cathode as the input signal. It should also be stressed that Z_n measured the lower of the two impedances, even if they were in series. Similar results already had been obtained during corrosion of Fe in Na_2SO_4 when a V_{bias} of 100 mV was applied.⁴ At frequencies higher than 100 Hz, Z_n approached $|Z_c|$ because of the instrumentation noise, as already observed.¹³ At intermediate frequencies (1 Hz to 100 Hz), the slight discrepancy between Z_n and $|Z_a|$ probably came from the evolution with time of the electrode impedance during the experiment,¹² or from the current noise i_a induced by the evolution of the few bubbles on the anodic side.

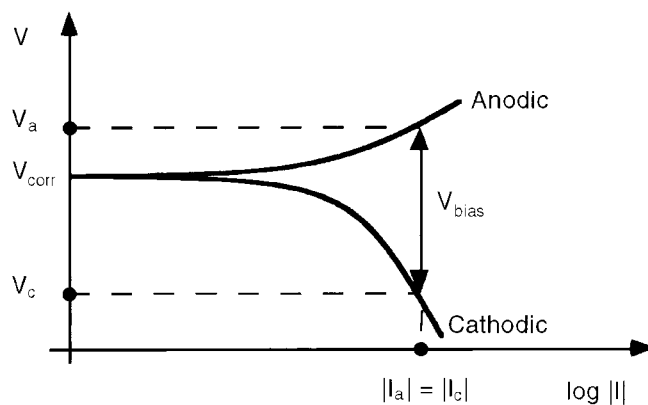


FIGURE 13. Current-voltage curve showing the potentials V_a , V_c of two identical corroding electrodes connected through a ZRA when a V_{bias} is superimposed.

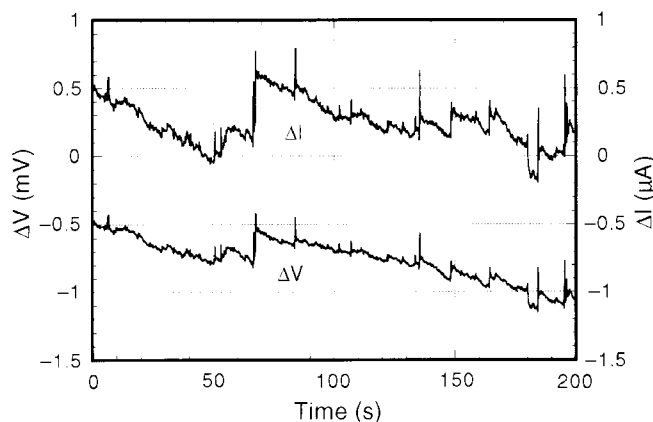


FIGURE 14. Time records of the voltage and current fluctuations generated during general corrosion of a low-carbon steel in 0.1 M $C_6H_8O_7$. A bias voltage of 350 mV was imposed between the two electrodes (diameter: 0.6 cm). Zeros of scales are arbitrary.

CONCLUSIONS

- ❖ The analysis of EN, begun a few decades ago, only recently has been introduced as a method for assessing and monitoring corrosion. The pioneering work of Eden, et al., has been instrumental in introducing the idea of a corrosion cell on which current and voltage fluctuations were measured.¹ The question remained of putting the interpretation of the data on a firm basis. This is now possible, so that the working of symmetrical and asymmetrical cells can be analyzed with confidence.
- ❖ Utilizing Equation (3), the results of EN measurements in quite different conditions can be understood and interpreted exactly. An intuitive description of the functioning of such a corrosion cell is that the noise generated by one of the electrodes acts as a source signal for the measurement of the impedance of the other electrode. The measurement

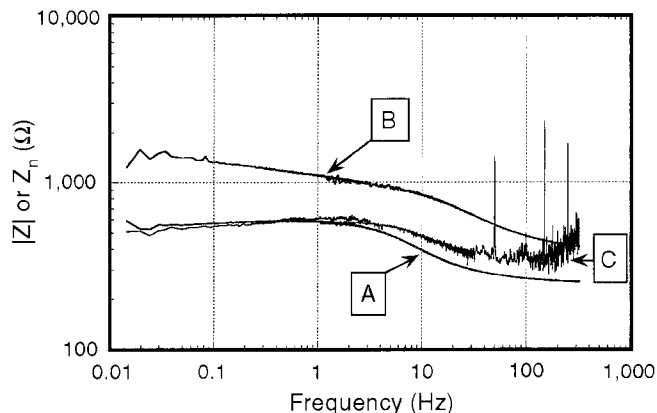


FIGURE 15. Impedance moduli of the: (A) anode, (B) cathode, and (C) noise impedance measured in the conditions of Figure 14.

of the impedance by means of an external broadband excitation is certainly not new,¹⁴ but in the EN case, the source is internal, which considerably simplifies the instrumentation necessary and makes its application for online corrosion monitoring attractive.

❖ A part of the information contained in the classical impedance measurement, however, is lost. This is the phase since Z_n is a real quantity (impedance modulus). In principle, if the measurement of Z_n is made over a very large frequency range, phase information could be recovered through a mathematical transformation of the Kramers-Kronig type, but, given the relatively poor signal-to-noise ratio of EN measurements, it is doubtful that such a scheme is of practical use.

❖ The above-mentioned intuitive description of the measurement of Z_n is also useful for assessing the possibility to use cells made asymmetric on purpose. If, to simplify, one of the corroding electrodes is substituted with an inert one (whether a microelectrode or a large one), it is unlikely that such an arrangement will be satisfactory for Z_n measurements because, in most cases, the inert electrode will be almost noiseless, and the measurement will generally produce the impedance of the inert electrode, with the corroding electrode as the noise-generating element.

❖ This analysis has shown that the measurements on asymmetrical cells can be analyzed and understood. This is encouraging since many corrosion cells, originally symmetrical, tend to become asym-

metrical with time, but nevertheless can yield useful information. Also, the technique of biasing the cell, so as to physically separate the anodic from the cathodic processes, might be exploited with success in many electrochemical systems.

❖ Although R_n is, in many cases, equal to the R_p of the electrodes under investigation, this is not always the case, even for symmetric systems.^{4-5,9} For asymmetric cells, its significance is doubtful. In analogy with the results of the analysis of Z_n in the same systems, it is likely that R_n too would give values close to the R_p of the less noisy electrode.

ACKNOWLEDGMENTS

A. Aballe and A. Bautista acknowledge the Ministry of Education and Culture of Spain for the grants that have allowed their participation in this work.

REFERENCES

1. D.A. Eden, K. Hladky, D.G. John, J.L. Dawson, "Electrochemical Noise—Simultaneous Monitoring of Potential and Current Noise Signals from Corroding Electrodes," CORROSION/86, paper no. 274 (Houston, TX: NACE International, 1986).
2. J.R. Kearns, J.R. Scully, P.R. Roberge, D.L. Reichert, J.L. Dawson, eds., ASTM STP 1277, "Electrochemical Noise Measurement for Corrosion Applications" (West Conshohocken, PA: ASTM, 1996).
3. U. Bertocci, C. Gabrielli, F. Huet, M. Keddad, J. Electrochem. Soc. 144, 1 (1997): p. 31.
4. U. Bertocci, C. Gabrielli, F. Huet, M. Keddad, P. Rousseau, J. Electrochem. Soc. 144, 1 (1997): p. 37.
5. F. Mansfeld, C.C. Lee, J. Electrochem. Soc. 144, 6 (1997): p. 2,068.
6. J.F. Chen, W.F. Bogaerts, Corrosion 52, 10 (1996): p. 753.
7. M.L. Benish, J. Sikora, B. Shaw, E. Sikora, M. Yaffe, A. Krebs, G. Martinchek, "A New Electrochemical Noise Technique for Monitoring the Localized Corrosion of 304 Stainless Steel in Chloride-Containing Solutions," CORROSION/98, paper no. 370 (Houston, TX: NACE, 1998).
8. F. Huet, U. Bertocci, C. Gabrielli, M. Keddad, "Noise Measurement in Corrosion," Proc. CORROSION/97, Research Topical Symposia (Houston, TX: NACE, 1997), p. 11.
9. A. Bautista, F. Huet, J. Electrochem. Soc. 146, 5 (1999): p. 1,730.
10. A. Bautista, H. Bertocci, F. Huet, "Influence of the Asymmetry in the Working Electrodes on Noise Resistance Measurements," 198th Meeting of the Electrochemical Society, abstract no. 354 (Pennington, NJ: Electrochemical Society, 2000).
11. F. Mansfeld, C. Chen, C.C. Lee, H. Xiao, Corros. Sci. 38, 3 (1996): p. 497.
12. A. Aballe, F. Huet, "Partition of Current Fluctuations in Noise Resistance Measurements," 198th Meeting of the Electrochemical Society, abstract no. 358 (Pennington, NJ: Electrochemical Society, 2000).
13. U. Bertocci, F. Huet, J. Electrochem. Soc. 144, 8 (1997): p. 2,786.
14. S.C. Creason, D.E. Smith, J. Electroanal. Chem. 36 (1972): Appendix I.